Polymorph Formation Studied by 3D Nucleation Simulations. Application to a Yellow Isoxazolone Dye, Paracetamol, and L-Glutamic Acid

Menno A. Deij,[†] Joop H. ter Horst,[‡] Hugo Meekes,*[,†] Peter Jansens,[‡] and Elias Vlieg[†]

IMM Solid State Chemistry, Faculty of Science, Radboud University Nijmegen, Toernooiveld 1, NL-6525 ED Nijmegen, The Netherlands, and Process & Energy Laboratory, Delft University of Technology, Leeghwaterstraat 44, NL-2628 CA Delft, The Netherlands

Received: October 3, 2006; In Final Form: December 12, 2006

Knowledge of the nucleation and growth behavior of polymorphs is vital in a variety of industrial applications. With the aid of the growth probability method the nucleus size is obtained as a function of the driving force for crystallization by simulating the growth probability of clusters of various sizes. From these values the cluster interfacial energy can be computed, allowing for the determination of the nucleation rate. The simulations show that nucleation of the metastable form of a yellow isoxazolone dye dominates at higher driving forces while below a certain driving force the stable form nucleates. Two other compounds show dominant nucleation of their stable form, even at extreme driving forces. This is in accordance with experimental findings for all these compounds. The growth probability method is therefore a promising indicator for polymorph nucleation behavior.

1. Introduction

Organic materials, like pharmaceuticals, dyes, and other compounds, may crystallize in multiple crystal structures called polymorphs. For applications it is essential to control this behavior and to select a specific polymorph, but it remains difficult to predict the relevant parameter values for that. The formation of different polymorphs depends on a number of parameters, the rate of nucleation being an important one. A commonly used rule for polymorph formation is Ostwald's rule of stages, which states that during the formation of a crystalline phase, the thermodynamically least stable phase forms first, which later transforms into the most stable phase, possibly through phases of intermediate stability.[1] There are, however, examples known of systems that do not follow this rule of stages, and it is generally accepted that the rule indeed does not apply to every system, for instance in the case where polymorphs nucleate at the same time, i.e., concomitantly.[2]

Nucleation of polymorphic systems has been studied computationally for simple models[3] and for the small molecules nitrogen and carbon dioxide.[4,5] Also in these studies, Ostwald's rule is not always obeyed[4] as the molecular dynamics (MD) simulations of carbon dioxide crystallization show that it crystallizes directly into its most stable polymorph.

More complex, organic crystals are still beyond the scope of MD simulations due to the computational cost involved. Therefore, in this paper we combine two relatively fast methods, Monte Carlo simulations of crystal growth and a growth probability method, and apply these methods to complex crystalline systems showing polymorphism. The combination of the two methods enables us to study the growth probability of small crystalline clusters for different polymorphic systems as a function of driving force for crystallization, $\Delta\mu/kT$. This leads to a prediction of the driving force dependence of the nucleation rate of each polymorph. The method will lead to a prediction of the conditions under which certain polymorphs can be produced and concomitant nucleation can be prevented and thus to an a priori product quality prediction.[6]

It will be shown that the growth probability can be used to determine the nucleus size as a function of the driving force for crystallization in the case of 3D homogeneous nucleation. The growth probability method has been used to study homogeneous nucleation of a liquid droplet in a vapor,[7] 2D nucleation of simple model systems,[8] and a theoretical study on homogeneous nucleation of terephthalic acid polymorphs,[6] using a modified Kossel model. In the current paper the growth probability method is combined with a Monte Carlo routine that can handle real crystal structures and is applied to three dimorphic systems: a yellow isoxazolone dye, paracetamol, and L-glutamic acid.

2. Theoretical Background

2.1. Nucleation Work. The nucleation rate J is the number of crystals generated per unit of time and volume and is according to classical nucleation theory (CNT) given by[9]

$$J = zf^*C_0 \exp\left(-\frac{W^*}{kT}\right) \tag{1}$$

where z is the Zeldovich factor, f^* is the attachment frequency of molecules to the nucleus, C_0 is the concentration of nucleation sites, W^* is the nucleation work, k is the Boltzmann constant, and T is the temperature. To predict the nucleation rate, an accurate prediction of the nucleation work W^* is required.

The work W for creating a cluster of size n is given by

$$W = -n\Delta\mu + \phi(n) \tag{2}$$

* Address correspondence to this author. E-mail: hugo.meekes@science.ru.nl.
[†] Radboud University Nijmegen.
[‡] Delft University of Technology.

10.1021/jp066509j CCC: $37.00
Published on Web 02/01/2007

in which $\phi(n)$ is the excess free energy of the n-sized cluster. This quantity is generally expressed as

$$\phi(n) = A_n\sigma_n = c_n\sigma_n(v_0 n)^{2/3} \tag{3}$$

with the interfacial energy σ_n of an n-sized cluster, A_n the surface area, v_0 the molecular volume, and c_n a numerical shape factor, which for a spherical cluster is equal to $(36\pi)^{(1/3)}$ and for a cubic cluster is equal to 6.

In case of a crystalline compound, however, the interfacial energy is anisotropic with respect to the surface orientation. The excess energy of a crystalline cluster is therefore a weighed average of the surface energy of all interfacial orientations present on the cluster. To describe nucleation behavior it is then more convenient to use a reduced nucleation parameter Γ as the weighed sum over all interfaces i, with interfacial energy σ_i and weight c_i, at the cluster surface.[10]

$$\phi(n) = \sum_i c_i\sigma_i(v_0 n)^{2/3} = \Gamma n^{2/3} \tag{4}$$

This nucleation parameter thus contains the interfacial energy and the shape factor. In CNT, these are, for homogeneous nucleation, assumed to be constant with respect to cluster size and equal to σ_∞ and c_∞, respectively, i.e., they are not a function of orientation, n, or $\Delta\mu$ and have the same value as that of a macroscopically large crystal. The nucleation parameter is therefore assumed to be constant as well. Setting dW/dn to zero and solving for the cluster with critical size n^* (i.e., the nucleus) results in the Gibbs−Thomson equation:

$$n^* = \frac{8}{27}\left(\frac{\Gamma}{kT}\frac{kT}{\Delta\mu}\right)^3 = \frac{8v_0^2}{27}\left(\frac{c_\infty\sigma_\infty}{\Delta\mu}\right)^3 \tag{5}$$

which describes the nucleus size n^* as a function of the nucleation parameter and the driving force. For homogeneous nucleation the nucleation work, $W^* = W(n^*)$, has a very simple relation with $\Delta\mu/kT$ in CNT:

$$\frac{W^*}{kT} = \frac{1}{2}n^*\frac{\Delta\mu}{kT} \tag{6}$$

2.2. The Growth Probability Method. A given cluster of n molecules changes its size randomly as a result of successive attachments and detachments. As these are random events, a given n-sized cluster can grow and reach macroscopic size only with a certain probability $P(n)$.[7] This growth probability of an n-sized cluster is a function of the cluster size n and the nucleus size n^*, and a numerical factor β between 0 and 1 and is given by

$$P(n) = \frac{1}{2}[1 + \mathrm{erf}(\beta(n - n^*))] \tag{7}$$

The numerical factor β is related to the Zeldovich factor z, which is present in the pre-exponential factor in the nucleation rate equation, according to

$$\beta = \pi^{1/2}z \tag{8}$$

For 3D homogeneous nucleation, CNT gives an expression for β[9]

$$\beta = \left(\frac{\Delta\mu}{6kTn^*}\right)^{1/2} \tag{9}$$

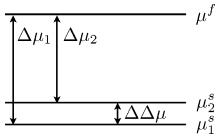

Figure 1. The definition of the various $\Delta\mu$ values for different polymorphs

By determining the growth probability as a function of the initial cluster size, n, and the dimensionless driving force for crystallization, $\Delta\mu/kT$, the nucleus size can be determined as a function of $\Delta\mu/kT$. With the aid of eq 6 an estimate of the nucleation work W^* can be made. The nucleation work is then used to calculate nucleation rates by using eq 1. As no information is known about the pre-exponential factors f^* and C_0 in eq 1, they are assumed to be constant and equal for both polymorphs (i.e., $f_1^* = f_2^*$ etc). Being pre-exponential, they will only weakly depend on $\Delta\mu/kT$.

2.3. Comparing Different Polymorphs. The driving force for crystallization, $\Delta\mu$, is given by the difference in chemical potential between molecules in the fluid phase and molecules in the solid phase:

$$\Delta\mu = \mu^f - \mu^s \tag{10}$$

such that when $\Delta\mu$ is positive, crystallization will take place. Now, when comparing two or more polymorphs, the chemical potential in the solid phases is different. For a dimorphic system at a certain concentration in the solution, we can write:

$$\Delta\mu_1 = \mu^f - \mu_1^s \tag{11}$$

$$\Delta\mu_2 = \mu^f - \mu_2^s \tag{12}$$

This means that experimentally, at a given solution concentration, molecules experience a different driving force for crystallization toward the stable phase 1 compared to the metastable phase 2. A clear example can be given when $\Delta\mu_1$ is taken to be positive and $\Delta\mu_2$ negative: the metastable polymorph will dissolve while the stable polymorph is formed. If we want to compare the outcome of the growth probability method for two polymorphs, we have to adjust for this difference. To express $\Delta\mu_1$ and $\Delta\mu_2$ by a single driving force $\Delta\mu$, in accordance with eqs 11 and 12, they are represented as (see also Figure 1):

$$\Delta\mu_1 = \Delta\mu$$

$$\Delta\mu_2 = \Delta\mu - \Delta\Delta\mu \tag{13}$$

where $\Delta\mu \equiv \mu^f - \mu_1^s$ and $\Delta\Delta\mu \equiv \mu_2^s - \mu_1^s$. With this representation of $\Delta\mu_1$ and $\Delta\mu_2$, the nucleation rates of both polymorphs at a given $\Delta\mu$ value can be compared as if it were an experiment at a given concentration, where each polymorph experiences its own supersaturation. The difference in $\Delta\mu$ is approximated by the difference in heat of dissolution, $\Delta_{\mathrm{diss}}H$, for both polymorphs. The results of the simulations (see Section 5) are displayed by using this correction in $\Delta\mu$ for the nucleus size as a function of $\Delta\mu$.

3. Methods

3.1. Simulating Cluster Growth. To simulate 3D nucleation for any crystal structure, the Monte Carlo crystal growth simulation program Monty[11] was adapted to simulate 3D nucleation. This program simulates crystal growth in a lattice system, based on a graph representation of the crystal structure

(see Section 3.2), that is, it is assumed that the clusters in the nucleation stage already have the crystallographic structure of the bulk crystal phase.

Originally, Monty was intended to be used for simulating crystal growth on specific crystallographic orientations (*hkl*).[11−15] To this end, a simulation box is created from a number of unit cells. Periodic boundary conditions are applied in the *a*- and *b*-direction; growth takes place in the *c*-direction. The initial starting configuration is a number of crystalline layers onto/from which growth units (GUs) can attach/detach. To simulate 3D nucleation, the two-dimensional periodic boundary conditions are removed, and the initially empty simulation box is taken suitably large, to avoid growth beyond the boundaries. An initial cluster of predetermined size is placed in the center of the simulation box and a simulation is run. To get an initial cluster of certain size the method uses an initialization routine that builds the cluster starting from a single GU. All the neighboring GUs that this GU connects to, i.e., has bonds to, are consecutively added. Next, all their neighbors are added, and so on, until the desired cluster size is reached. Generally, this leads to a more or less spherical cluster.

Next, to find the energetically optimal shape of the cluster under the simulation conditions chosen, each simulation run is preceded by an equilibration simulation with a constant number of GUs, using a Metropolis-type algorithm.[16,17] Briefly, at each Monte Carlo move a randomly selected GU is moved to a different location on the initial cluster according to the following conditions

$$\Delta E = E_{\text{final}} - E_{\text{initial}} = \begin{cases} < 0 & \text{move accepted} \\ > 0: & e^{-\Delta E/kT} \begin{cases} > R & \text{move accepted} \\ < R & \text{move rejected} \end{cases} \end{cases} \quad (14)$$

in which R is a random number between 0 and 1. The difference in energy is calculated from the final (E_{final}) and initial (E_{initial}) energies following from the respective broken bond configurations of the GU being moved. These and subsequent simulations are all run at 300 K, which is representative enough for typical solution growth situations.

After the equilibration run, a simulation run is performed at a specific driving force by using the original Monty event algorithm, which uses an *n*-fold way algorithm.[11,18] This algorithm was chosen for efficiency, as at each Monte Carlo event, a move will be accepted. In contrast, for a Metropolis-type algorithm, moves are not accepted when the conditions for that move are not met. For crystal growth, especially at low driving force, the growth is often limited by a barrier for nucleation. Using a Metropolis algorithm in that case could result in most attempted moves being rejected, which would lead to very long simulation times.

A simulation run is stopped if the cluster is reduced to a size of a single GU (the cluster decays) or when the cluster has reached a size for which the growth probability, determined in earlier simulations, is unity (the cluster grows out). For a specific initial cluster size n at a certain driving force, the growth probability is given by the fraction of successful simulation runs. For each initial cluster size, at least 500 simulation runs are performed. Fitting the growth probabilities for different initial cluster sizes determined at a given driving force to eq 7 results in the nucleus size n^* as well as β at that driving force. These values can then be used together with eqs 6 and 1 to calculate the nucleation rate as a function of the driving force.

TABLE 1: Crystal Graph Bonds with Respect to Vacuum of the Isoxazolone Dye Form I (left) and II (right)[a]

form **I**		form **II**	
bond	bond energy [kcal·mol^{-1}]	bond	bond energy [kcal·mol^{-1}]
1−3[$\bar{1}\bar{1}$1]	−21.05	1−2[010]	−22.00
1−4[$\bar{1}$00]	−8.81	1−2[000]	−18.72
1−2[$\bar{1}$10]	−7.07	1−4[$\bar{1}$00]	−6.44
1−3[$\bar{1}$01]	−6.33	2−4[$\bar{1}$10]	−6.39
1−3[0$\bar{1}$1]	−3.56	1−4[000]	−5.16
1−2[000]	−3.55	1−4[$\bar{1}$01]	−3.38
1−1[100]	−2.64	1−3[000]	−3.33
1−4[$\bar{1}$10]	−2.21	1−3[$\bar{1}$00]	−2.86
		1−4[$\bar{1}\bar{1}$0]	−2.21

[a] The first entry in the left table is read as a bond that goes from GU 1 to GU 3, translated along [$\bar{1}\bar{1}$1] on the lattice basis.

3.2. Calculation of Crystal Graphs. The Monty program uses the crystal graph representation of a crystal structure. In a crystal graph the growth units (i.e., molecules, ions) are represented by graph vertices and the pairwise interactions between growth units are represented by graph edges. The graph edges' weight represents the strength of the interaction. To calculate the pairwise interactions between the molecules in the crystal structure, we use the Dreiding forcefield[19] in Cerius[2 20] with partial atomic charges calculated using a restricted electrostatic potential (RESP) fitting method.[21] We use this RESP method to come to a single set of partial atomic charges for all conformers of all polymorphs of a given molecule. Changing the conformation of a molecule is usually associated with a slight change in charge distribution. Having a single set of partial atomic charges for all conformations enables us to directly compare energies between the different polymorphs, instead of having to estimate or ignore the energy associated with a change in charge distribution.

The molecules' partial atomic charge distribution is calculated with respect to vacuum. After calculation of the charges, the molecules are placed at their original site in the crystal structure. The crystal structure geometry is then optimized by using Ewald summation for the van der Waals and Coulombic contributions. After this optimization, all pairwise interactions within a certain cutoff radius are calculated. The sum of all interactions is scaled to be equal to the enthalpy of dissolution of the particular polymorphic form; only scaled interactions that have a magnitude above kT are used in the crystal graph.

4. Crystal Structures and Crystal Graphs

4.1. Yellow Isoxazolone Dye. In a previous study, the polymorphic behavior of two polymorphs of an isoxazolone dye was studied experimentally as a function of the supersaturation.[22] It was found that the metastable polymorph **II** is kinetically favored, as a fast cooling rate exclusively leads to the formation of needle-like crystals of this polymorphic form. Lower driving forces combined with slow cooling rates yield the stable polymorphic form **I**. The crystal morphologies were studied experimentally and compared to 2D nucleation crystal growth simulations done with Monty and they were found to correspond well[14] so that this system was an obvious choice to use in the study of the 3D growth probability. The crystal graph of this study was used unaltered here: the crystal graph details are listed in Table 1. For comparison of the two polymorphs a value of $\Delta\Delta\mu$ of 1.6kT was used, as the dissolution enthalpies differ by 1 kcal·mol^{-1}.[22]

4.2. Paracetamol. Paracetamol, a well-known analgesic drug, is used worldwide in the production of pain-relief tablets. It

TABLE 2: Experimental and Optimized Lattice Parameters for Two Polymorphs of Paracetamol (spacegroup $P2_1/a$ with $Z = 4$ and $P2_1/a2_1/b2_1/c$ with $Z = 8$) and Two Polymorphs of L-Glutamic Acid (both forms with spacegroup $P2_12_12_1$ and $Z = 4$)

crystal structure	a (Å)	b (Å)	c (Å)	β (deg)
paracetamol (monoclinic)				
HXACAN01	12.93	9.40	7.10	115.9
optimized	13.24	9.30	7.27	117.5
paracetamol (orthorhombic)				
HXACAN08	7.41	11.84	17.16	
optimized	7.24	12.06	17.26	
L-glutamic acid (α)				
LGLUAC03	10.28	8.78	7.07	
optimized	10.34	8.49	7.87	
L-glutamic acid (β)				
LGLUAC11	5.16	17.30	6.95	
optimized	5.19	17.85	6.78	

TABLE 3: Crystal Graph Bonds with Respect to Vacuum of Monoclinic (left) and Orthorhombic Paracetamol (right)

monoclinic paracetamol (**I**)		orthorhombic paracetamol (**II**)	
bond	bond energy [kcal·mol^{-1}]	bond	bond energy [kcal·mol^{-1}]
1−1[001]	−2.35	1−3[000]	−4.28
1−2[$0\bar{0}0$]	−4.01	1−4[$0\bar{0}0$]	−3.10
1−3[$1\bar{1}1$]	−3.91	1−5[$\bar{1}00$]	−7.21
1−3[100]	−2.80	1−5[000]	−6.04
1−3[101]	−8.81	1−6[000]	−8.24
1−4[101]	−9.90	1−7[000]	−9.63
1−4[000]	−9.41	1−8[000]	−2.53

has also become a well-studied pharmaceutical solid. Three polymorphs are known, of which the stable monoclinic form **I** is marketed worldwide. The orthorhombic form **II**[23−25] is interesting for pharmaceutical applications, as its tabletting properties are superior to those of form **I**. The third polymorph is very unstable, and its structure has not been determined experimentally. Recently a number of likely structures were determined computationally by using polymorph prediction,[26] and one of the predicted structures (AK6) "gave a calculated powder pattern that closely matched the observed powder pattern for form **III**".[27] In the present study we consider forms **I** and **II**.

As the enthalpy of dissolution in water is only known for form **I**, it is estimated for form **II** by subtracting the difference in enthalpy of fusion:

$$\Delta_{diss}H(\mathbf{II}) \approx \Delta_{diss}H(\mathbf{I}) - \Delta\Delta_{fus}H$$

With use of this simple equation, the two enthalpies of dissolution in water used are 5.37 and 5.01 kcal·mol^{-1} for forms **I** and **II**, respectively, calculated by using the enthalpies of fusion of 6.92 and 6.56 kcal·mol^{-1}, respectively.[28] Therefore, a value for $\Delta\Delta\mu$ of 0.36 kcal·mol^{-1}, or 0.6kT, was used.

The crystal structures of paracetamol (Cambridge Structural Database reference codes HXACAN01 and HXACAN08) were minimized by using the procedure outlined before. The results of the minimization and the crystal graph are listed in Tables 2 and 3.

4.3. L-Glutamic Acid. L-Glutamic acid is an amino acid industrially prepared by fermentation. It is a well-studied polymorphic compound with two distinct polymorphs, α and β. The metastable α form has a prismatic crystal morphology, whereas the stable β form has an elongated plate-like shape.

The dissolution enthalpy was measured by Sakata et al. to be 5.55 kcal·mol^{-1} for the α form and 5.15 kcal·mol^{-1} for the β form. This leads to a $\Delta\Delta\mu$ difference of 0.67kT when comparing the two polymorphs.

TABLE 4: Crystal Graph Bonds with Respect to Vacuum of L-Glutamic Acid α (left) and β (right)

L-glutamic acid α form		L-glutamic acid β form	
bond	bond energy [kcal·mol^{-1}]	bond	bond energy [kcal·mol^{-1}]
1−2[000]	−32.90	1−2[$\bar{1}\bar{1}0$]	−29.39
1−3[000]	−15.97	1−2[$0\bar{1}0$]	−23.61
1−4[000]	−24.01	1−3[000]	−17.94
1−4[010]	−11.55	1−4[001]	−6.35
1−1[011]	−2.27	1−1[$\underline{1}00$]	−8.81
1−1[$01\underline{0}$]	−2.35	1−2[$\bar{1}\bar{1}1$]	−2.62
1−4[$01\bar{1}$]	−2.79	1−3[001]	−3.39

The crystal structures of L-glutamic acid (LGLUAC03 and LGLUAC11) were minimized by using the procedure outlined before. The original and minimized lattice parameters are listed in Table 2. All optimized lattice parameters are within 5% of the original lattice parameters, except for the optimized c-axis of the α form of L-glutamic acid that changed 11% in length. The crystal graph bonds are listed in Table 4.

5. Results and Discussion

5.1. Equilibration of Clusters of the Isoxazolone Dye Polymorphs. The simulation procedure starts with the equilibration of the initial cluster. To illustrate the benefits and necessity of this equilibration step in the simulation procedure, clusters of the two polymorphs of the yellow isoxazolone dye with an initial size of 100 GUs were equilibrated and then grown out to a final size of 300 GUs. The results are displayed in Figure 2. In the figure the initial, equilibrated, and final cluster shapes are displayed. It can be seen that the initial cluster for polymorph **II** contains more kink sites, compared to the equilibrated cluster. For polymorph **I** the cluster has a less spherical shape, compared to the equilibrated cluster. The grown clusters show the difference in growth morphology: polymorph **I** has a final shape as indicated by the thin black lines in the figure and polymorph **II** has a needle shape; it effectively only grew in the needle direction.

5.2. Fitting of the Simulation Results for L-Glutamic Acid. After the equilibriation stage at a constant number of GUs at each value for the driving force the cluster is left to grow or decay. The probability for either of these two events is fitted to eq 7. The result of such a fit is shown for both polymorphs of L-glutamic acid in Figure 3.

5.3. Nucleation of the Yellow Isoxazolone Dye Polymorphs. The nucleation results for polymorphs **I** and **II** are shown in Figures 4 and 5. A clear difference can be observed as the metastable polymorph **II** nucleates at lower $\Delta\mu/kT$ than the stable polymorph **I**. In Figure 4, the solid lines show a fit to the Gibbs−Thomson eq 5. The values for Γ/kT (see eq 5), resulting from the fit, are listed in Table 5. In Figure 5 the nucleation rates are plotted by using the fit results of the simulation data to eq 7 together with eqs 1 and 6. The solid lines in this figure use the fits of Figure 4 and an averaged value for the Zeldovich factor $z = \beta\pi^{-1/2}$. The value at which the extrapolated lines cross lies around $\Delta\mu = 2.5kT$, which is still larger than the value of $\Delta\mu = \Delta\Delta\mu = 1.6kT$ for which the bulk metastable polymorph is in thermodynamic equilibrium with a saturated solution. This shows that for driving force values $1.6kT < \Delta\mu < 2.5kT$ the stable polymorph has a larger nucleation rate, although the nucleation rates are probably too small to be of practical relevance.

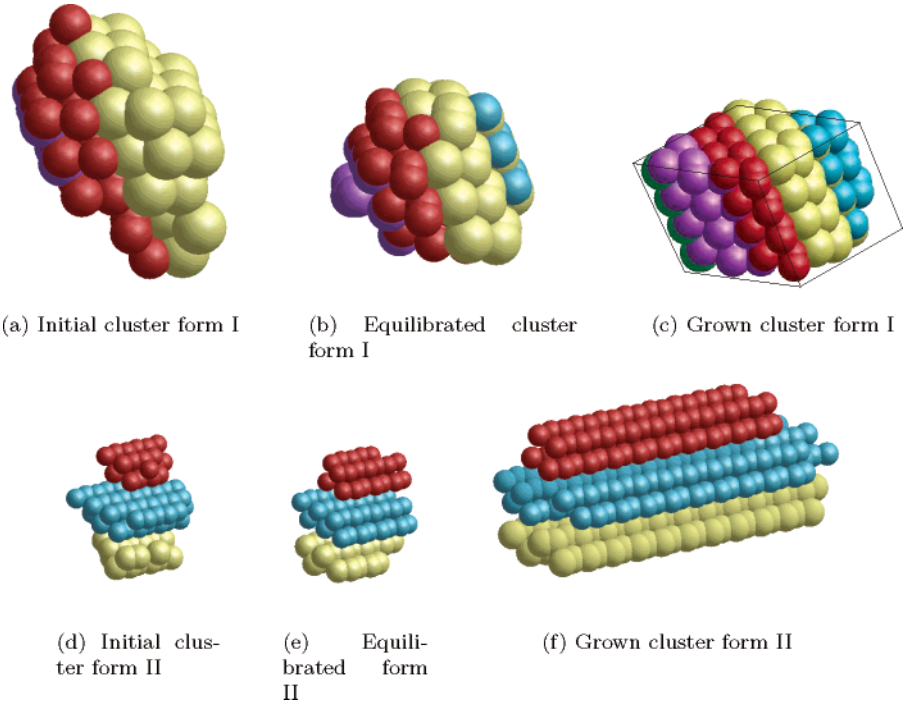

(a) Initial cluster form I (b) Equilibrated cluster form I (c) Grown cluster form I

(d) Initial cluster form II (e) Equilibrated form II (f) Grown cluster form II

Figure 2. Initial, equilibrated, and grown clusters of two polymorphs of the yellow dye. The colors of the GUs are merely there to make it easier to see structure in the clusters.

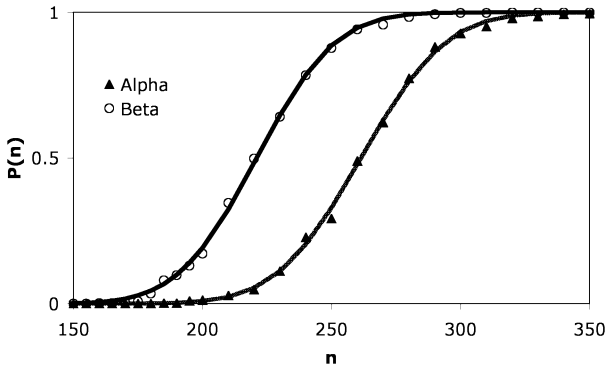

Figure 3. Simulation results for the growth probability $P(n)$ as a function of the initial cluster size n for both polymorphs of L-glutamic acid at a driving force of $\Delta\mu/kT = 1.05$. The solid lines are fits to eq 7.

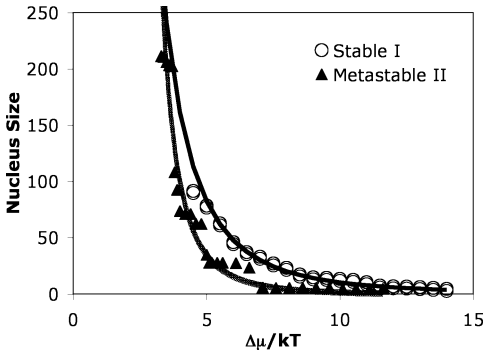

Figure 4. Nucleus size (i.e., the size of the critical cluster) for polymorphs **I** and **II** of the isoxazolone dye as a function of driving force $\Delta\mu/kT$. A value for $\Delta\Delta\mu$ of $1.6kT$ was used, shifting the metastable polymorph to higher $\Delta\mu/kT$ values. The fitted lines were obtained by using the Gibbs−Thomson eq 5 with Γ/kT as a fitting parameter.

There is a large difference in interfacial energy between the two polymorphic forms, which is caused by the fact that the metastable polymorph **II** has a needle-like morphology. Most of the surface of the needle is composed of crystallographic

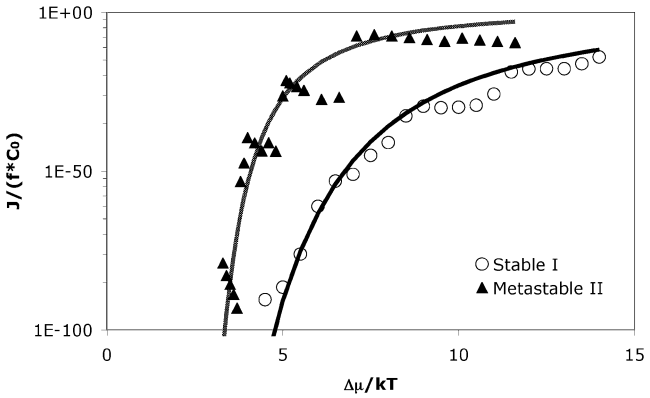

Figure 5. Nucleation rates for polymorphs **I** and **II** of the yellow dye. A value for $\Delta\Delta\mu$ of $1.6kT$ was used. The extrapolated fit lines cross at around $\Delta\mu/kT = 2.5$.

TABLE 5: Values of Γ/kT for Both Polymorphs of the Yellow Isoxazolone Dye

polymorph	Γ/kT
stable form **I**	32.67
metastable form **II**	16.76

orientations that have very low interfacial energy, as compared to the orientations at the needle tip. Consequently, a considerably lower Γ/kT value can be realized through the anisotropic shape. In contrast, for the stable polymorph **I**, there is not a particular orientation that has much lower interfacial energy and, therefore, its shape is more isotropic and the Γ/kT value higher. Thus the origin of the more favorable nucleation of the metastable phase is its lower surface energy due to its anisotropic shape.

The needle shape is probably also the cause for the large deviations of the simulation results from the fitted line in Figure 4. Forming steps and islands on the side faces of the needle is energetically very unfavorable. The deviations may therefore be a result of statistical fluctuations, but could also be caused by the starting configuration for the simulations, since the size of the side faces is a function of the initial cluster size, making

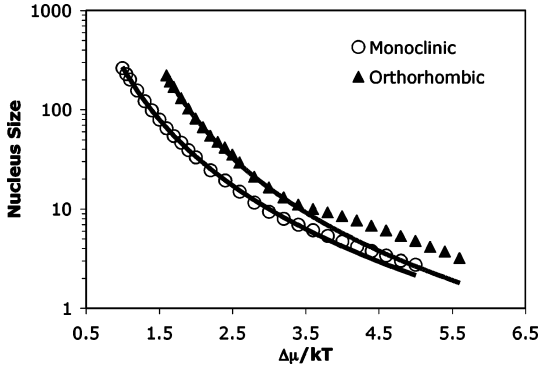

Figure 6. The nucleus size for two polymorphs of paracetamol. A value for $\Delta\Delta\mu$ of 0.6kT was used.

the behavior of the nucleus size with respect to $\Delta\mu/kT$ quite discontinuous.

During the simulation of the stable polymorph **I**, within 10^7 MC steps some simulation runs did not progress beyond certain cluster sizes, which were larger than the initial cluster, but smaller than clusters for which the growth probability was unity (i.e., the condition for successful nucleation and termination of the simulation run). Detailed inspection of these clusters showed that they corresponded to facetted nanocrystallites that did not grow further due to the 2D nucleation barrier on the facets of the crystallites (such a nanocrystallite is displayed in Figure 2c). These crystallites represent local minima in the free energy as a function of cluster size, and due to the energetics of the system result in a high 2D nucleation barrier. Simulation runs of clusters that did not grow out to their final size were taken to be successful. This may underestimate the nucleus size as a function of $\Delta\mu/kT$, but when looking at the results obtained for the stable polymorph of the yellow isoxazolone dye, this does not lead to a major shift in nucleation behavior. If anything, the curves in Figures 4 and 5 of polymorph **I** would be shifted to higher $\Delta\mu/kT$ values, making the difference between the two polymorphs even greater. This high 2D nucleation barrier for facetted nanocrystallites was not observed for any of the other systems studied.

5.4. Nucleation of Two Polymorphs of Paracetamol. Experimentally, the nucleation behavior in solution of paracetamol seems to favor the formation of the stable monoclinic form under all circumstances. The orthorhombic form can be obtained from the melt, and these crystals are used to seed solutions of paracetamol in benzyl alcohol and industrially methylated spirits.[23] The latter solvent was used to obtain laboratory-scale amounts of the orthorhombic form of paracetamol, but the yields were low, about 30%, as the monoclinic form started to crystallize at that point.

By using the same procedure as above, the nucleus size was determined and fitted to the Gibbs−Thomson equation (Figure 6). The nucleation rates are shown in Figure 7. It can be seen in the figure that the nucleation process favors the stable monoclinic form **I** over the metastable orthorhombic form **II**. Interestingly, in the high $\Delta\mu/kT$ region of the figure, which is displayed in Figure 7b, a clear deviation from the fitted line toward lower nucleation rates for the orthorhombic form can be seen, seemingly leading to non-crossing curves, even at high driving forces. This indicates that the assumption of constant interfacial energy with respect to the nucleus size, as implied in eq 5, does not hold for nuclei smaller than about 10 molecules. At the same time it also indicates that the classical nucleation theory holds, even down to a nucleus as small as 10 molecules. This deviation supports the difficulties in preparing

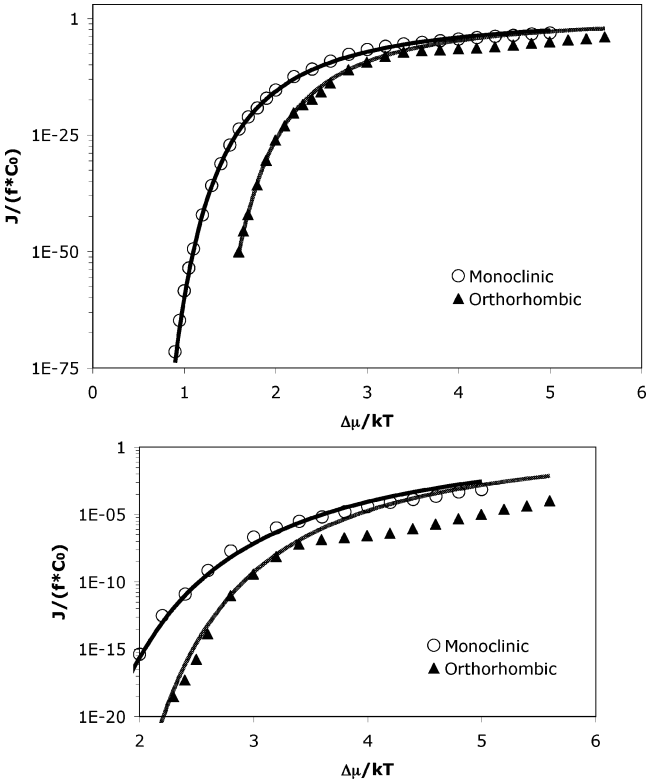

Figure 7. The nucleation rates for the two polymorphs of paracetamol. A value for $\Delta\Delta\mu$ of 0.6kT was used. The second graph shows a clear deviation to lower rates from the fitted line for the orthorhombic form at higher driving forces.

TABLE 6: Values of Γ/kT for Both Polymorphs of Paracetamol

polymorph	Γ/kT
monoclinic stable form **I**	9.68
orthorhombic metastable form **II**	9.95

orthorhombic paracetamol,[23] as it supports the claim that the orthorhombic form has a substantially higher nucleation barrier.

There is no significant difference in the Γ/kT values for both polymorphs (see Table 6), which means that the surface energy of the nucleus is not determining which polymorph is formed, but rather the different $\Delta\mu$ values for the two polymorphs. As a consequence, the orthorhombic form will not be formed easily.

5.5. Nucleation of the L-Glutamic Acid Polymorphs. The crystallization behavior of L-glutamic acid seems to depend mostly on stirring in the crystallization vessel. When a supersaturated solution is stirred, the metastable α polymorph forms mostly, whereas β forms in stagnant solutions.[29,30] This behavior is ascribed to the fact that α grows faster, whereas β has the higher nucleation rate. In a stirred solution, α crystals reach the critical size for attrition first, which results in a large number of secondary nuclei being formed, leading to the formation of α L-glutamic acid. In contrast, when the solution is not stirred, secondary nucleation does not take place, and β L-glutamic acid is formed. As the method used in this paper cannot simulate the effects of attrition, the results are thought to best represent the situation of a stagnant solution. There are also a number of reports that show the solution-mediated solid-state transformation of α to β, for instance in refs 31 and 32. The results of the growth probability method applied to the L-glutamic acid system are shown in Figures 8and 9 and it can be seen that, although the nucleus size as a function of $\Delta\mu/kT$ is not very different for the two polymorphs, the nucleation rates indicate that the formation of β L-glutamic acid is favored over

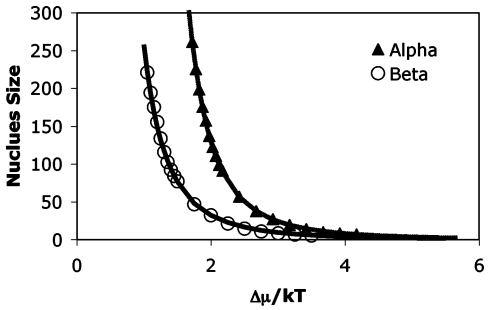

Figure 8. The nucleus size for two polymorphs of L-glutamic acid. A value for $\Delta\Delta\mu$ of 0.67kT was used.

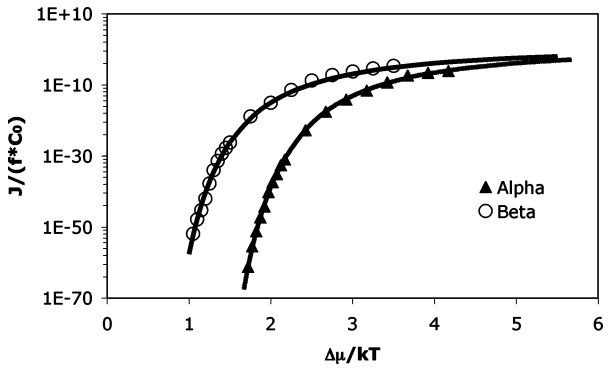

Figure 9. The nucleation rates for the two polymorphs of L-glutamic acid. A value for $\Delta\Delta\mu$ of 0.67kT was used.

TABLE 7: Values of Γ/kT for Both Polymorphs of L-Glutamic Acid

polymorph	Γ/kT
α metastable form	10.08
β stable form	9.54

the formation of the α form. There is no clear difference in the Γ/kT values for both polymorphs (see Table 7), again indicating the favorable formation of the stable polymorph directly, due to the difference in $\Delta\mu$.

In a recent paper, Hammond et al. present the results of the calculation of energies of clusters of various sizes of α and β L-glutamic acid.[33] Their method comprises the creation of clusters of various sizes in the shape of the macroscopic crystal, which was predicted by using the attachment energy method. Compared to our results, where the β form is formed directly, the results of that study are surprising, as they show that minimized clusters of less than 200 molecules and non-minimized clusters of less than 50 molecules of α L-glutamic acid have lower energy than those of β L-glutamic acid.[33] It seems reasonable, though, to include the statistical process of attachment and detachment of molecules in the determination of nucleation rates, as is done in the growth probability method. When this process is included, the results are indeed consistent with the direct formation of β L-glutamic acid from stagnant solutions.

5.6. The Role of $\Delta\Delta\mu$ and Γ. The main result of this paper is that the Γ/kT values can be determined from the simulations and the growth probability method. When the Γ/kT values of two polymorphs are comparable, the discriminating factor between polymorph nucleation rates is largely due to the $\Delta\Delta\mu$ term, as it is in the examples of paracetamol and L-glutamic acid. In other words, the difference in nucleation behavior is in that case not caused by a difference in surface energy, but only due to the difference in bulk chemical potential, $\Delta\Delta\mu$. It has been made clear that the $\Delta\Delta\mu$ term originates from the thermodynamic treatment of the system with two polymorphs forming in the same solution. Practically, the difference in $\Delta\mu$ was approximated by the difference in dissolution enthalpy, which can only be measured by using adequate samples of both polymorphs, in which case the simulations might be of reduced value for prediction of favorable conditions under which the polymorphs can be made, since by then experimental data are available. It has also been shown that the difference in enthalpy of fusion can be used when solution data are not available, which opens up the possibility of using, e.g., DSC data to come to an approximate $\Delta\Delta\mu$ value. By using DSC, different polymorphs and their heat of fusion may be obtained from interconversion or from cooling a molten sample, so this can be a situation in which these simulations have more practical value. Unfortunately, forcefields are generally not yet accurate enough to predict $\Delta\Delta\mu$ values or differences in dissolution enthalpy.

Polymorph formation, as studied in this paper, is thus governed by either a difference in bulk chemical potential or a difference in interfacial energy. It is useful to know which parameter is of influence, as differences in interfacial energies between polymorphs can be manipulated advantageously by choosing a solvent carefully. When bulk chemical potential is the dominant factor in polymorph nucleation, other routes toward polymorph selection may be applied. As an example, the case of L-glutamic acid demonstrates that although the nucleation rate of the β form is highest, the higher growth rate of the α form can be used to form that polymorph by ensuring that its nuclei reach their critical size for secondary nucleation first.

6. Conclusions

The use of the growth probability method for predicting 3D homogeneous nucleation rates has been highlighted by using three examples of experimentally well-characterized organic compounds. In all three cases the experimental crystallization behavior shows results similar to the simulations. In the first case, the metastable form of the yellow isoxazolone dye has a clear kinetic advantage compared to the stable polymorph at higher driving forces, which is in accordance with Ostwald's rule of stages. In this case the kinetic advantage is due to a lower interfacial energy of the nucleus of the metastable polymorph, that more than compensates the difference in bulk chemical potential. The two other cases, those of paracetamol and L-glutamic acid, show a behavior that is not consistent with Ostwald's rule, i.e., the stable polymorph is formed directly in favor of the metastable polymorph, both experimentally as well as in the simulations. For these cases the interfacial energies are comparable. The fact that the stable polymorph is formed in spite of the rule of stages can thus be explained in terms of the crystal structure, the interactions between growth units, driving force for crystallization, and the growth behavior of small crystalline clusters, which results in values for the Γ/kT parameter used in the description of nucleation. These parameters all seem to be important in the correct description of the problem; other factors like detailed kinetics of growth unit incorporation and solvent interactions can be neglected for the examples shown.

In the case where the difference in bulk chemical potential determines which polymorph is formed, the solvent interactions may indeed be neglected. In other cases, where the interfacial energy determines polymorph formation, solvents may be employed to modify interfacial energies in such a way that the formation of the desired polymorph can be promoted or other phenomena, like secondary nucleation, can be used to selectively form the desired polymorphic form.

The method is well-suited to be adopted in the screening of polymorphs and the determination of conditions for preparation of certain polymorphs. As it is known that polymorphs may nucleate concomitantly, the use of the method can help in determining conditions for which this unwanted behavior can be prevented. Also, in the computational prediction of polymorphism, the incorporation of nucleation behavior can give an additional tool to discriminate between the often large set of possible crystal structures.

Acknowledgment. The authors would like to thank Shanfeng Jiang for her contribution to the selection of polymorphic systems. One of us (M.D.) would like to thank Synthon B.V. for funding.

References and Notes

(1) Ostwald, W. *Z. Phys. Chem.* **1897**, *22*, 289−330.
(2) Bernstein, J.; Davey, R. J.; Henck, J.-O. *Angew. Chem., Int. Ed.* **1999**, *38*, 3440.
(3) van Duijneveldt, J. S.; Frenkel, D. *J. Chem. Phys.* **1992**, *96*, 4655−4668.
(4) Leyssale, J.-M.; Delhomme, J.; Millot, C. *J. Chem. Phys.* **2005**, *122*, 184518.
(5) Leyssale, J.-M.; Delhomme, J.; Millot, C. *J. Chem. Phys.* **2005**, *122*, 104510.
(6) ter Horst, J. H.; Kramer, H. J. M.; Jansens, P. J. *Chem. Eng. Technol.* **2006**, *29*, 175−182.
(7) ter Horst, J. H.; Kashchiev, D. H. *J. Chem. Phys* **2003**, *119*, 2241−2246.
(8) ter Horst, J. H.; Jansens, P. J. *Surf. Sci.* **2005**, *574*, 77−88.
(9) Kashchiev, D. *Nucleation, basic theory with applications*; Butterworth Heinemann: Oxford, UK, 2000.
(10) ter Horst, J. H.; Kramer, H. J. M.; Jansens, P. J. *Cryst. Growth Des.* **2002**, *2*, 351−356.
(11) Boerrigter, S. X. M.; Josten, G. P. H.; van de Streek, J.; Hollander, F. F. A.; Los, J.; Cuppen, H. M.; Bennema, P.; Meekes, H. *J. Phys. Chem. A* **2004**, *108*, 5894−5902.
(12) Cuppen, H. M.; Beurskens, G.; Kozuka, S.; Tsukamoto, K.; Smits, J. M. M.; de Gelder, R.; Grimbergen, R.; Meekes, H. *Cryst. Growth Des.* **2005**, *5*, 917−923.
(13) Cuppen, H. M.; van Eerd, A. R. T.; Meekes, H. *Cryst. Growth Des.* **2004**, *4* (5), 989−997.
(14) Deij, M. A.; Aret, E.; Boerrigter, S. X. M.; van Meervelt, L.; Deroover, G.; Meekes, H.; Vlieg, E. *Langmuir* **2005**, *21*, 3831−3837.
(15) Boerrigter, S. X. M.; Cuppen, H. M.; Ristic, R. I.; Sherwood, J. N.; Bennema, P.; Meekes, H. *Cryst. Growth Des.* **2002**, *2* (5), 357−361.
(16) Metropolis, N.; Rosenbluth, A. W.; Rosenbluth, M. N.; Teller, A. H.; Teller, E. *J. Chem. Phys.* **1953**, *21*, 1087−1092.
(17) Metropolis, N.; Ulam, S. *J. Am. Stat. Assoc.* **1949**, *44*, 335−341.
(18) Bortz, A. B.; Kaloz, M. H.; Lebowitz, J. L. *J. Comput. Phys.* **1975**, *17*, 10−18.
(19) Mayo, S. L.; Olafson, B. D.; Goddard, W. A., III *J. Phys. Chem.* **1990**, *94*, 8897−8909.
(20) *Cerius*^{2} *User Guide*; Accelrys Inc.: 9685 Scranton Road, San Diego, CA, 1997.
(21) Cornell, W. D.; Cieplak, P.; Bayly, C. I.; Kollman, P. A. *J. Am. Chem. Soc.* **1993**, *115*, 9620−9631.
(22) Aret, E.; Meekes, H.; Vlieg, E.; Deroover, G. *Dyes Pigm.* **2007**, *72*, 339−344.
(23) Nichols, G.; Frampton, C. S. *J. Pharm. Sci.* **1998**, *87*, 684−693.
(24) Haisa, M.; Kashino, S.; Maeda, H. *Acta Crystallogr., Sect. B*: *Struct. Crystallogr. Cryst. Chem.* **1974**, *30*, 2510.
(25) Mikhailenko, M. A. *J. Cryst. Growth* **2004**, *265*, 616−618.
(26) Beyer, T.; Day, G. M.; Price, S. L. *J. Am. Chem. Soc.* **2001**, *123*, 5086−5094.
(27) Peterson, M. L.; Morissette, S. L.; McNulty, C.; Goldswweig, A.; Shaw, P.; LeQuesne, M.; Monagle, J.; Encina, N.; Marchionna, J.; Johnson, A.; Gonzalez-Zugasti, J.; Lemmo, A. V.; Ellis, S. J.; Cima, M. J.; Almarsson, O. *J. Am. Chem. Soc.* **2002**, *124*, 10958−10959.
(28) Espeau, P.; Ceolin, R.; Tamarit, J.-L.; Perrin, M.-A.; Gauchi, J.-P.; Leveiller, F. *J. Pharm. Sci.* **2005**, *94*, 524−539.
(29) Roelands, C. P. M.; ter Horst, J. H.; Kramer, H. J. M.; Jansens, P. J. *J. Cryst. Growth* **2005**, *275*, e1389−e1395.
(30) Kitamura, M. *J. Cryst. Growth* **1989**, *96*, 541−546.
(31) Ferrari, E. S.; Davey, R. J. *Cryst. Growth Des.* **2004**, *4*, 1061−1068.
(32) Ono, T.; Kramer, H. J. M.; ter Horst, J. H.; Jansens, P. J. *Cryst. Growth Des.* **2004**, *4*, 1161−1167.
(33) Hammond, R. B.; Pencheva, K.; Roberts, K. J. *J. Phys. Chem. B* **2005**, *109*, 19552.